Chapter

Synthesis of Curved Surface Plasmon Fields through Thin Metal Films in a Tandem Array

Gabriel Martinez Niconoff, Marco Antonio Torres Rodriguez, Mayra Vargas Morales and Patricia Martinez Vara

Abstract

We describe the generation of plasmonic modes that propagate in a curved trajectory inducing magnetic properties. This is performed by masking a metal surface with two screens containing a randomly distributed set of holes that follow a Gaussian statistic. The diameter of the holes is less than the wavelength of the illuminating plane wave. By implementing scaling and rotations on each screen, we control the correlation trajectory and generate long-range curved plasmonic modes. Using the evanescent character of the electric field, the study is implemented for the transmission of a plasmonic mode propagating in a tandem array of thin metal films offering the possibility to generate localization effects.

Keywords: plasmon mode, surface plasmon field, speckle, thin films, curved correlation trajectory

1. Introduction

During the last decade, the scientific community has shown an increasing interest in the models of plasmon fields due to their potential applications, which occur practically in all branches of science and technology. In the present study, we emphasize the analysis of correlation trajectories on a metal surface with random structure. The resulting model offers applications to development of nano-antennas having the possibility of a tunable bandwidth [1]. This type of structure has applications in the synthesis of new light sources and the control of magnetic effects [2]. The tunable effects are controlled with the curvature parameter having applications in surface-enhanced Raman spectroscopy (SERS), also as the local excitation of quantum dots. Implementing the evanescent behavior of the plasmon field, the analysis is extended to the propagation of plasmon fields through a tandem array of metal films similar to photonic crystal structures [3, 4].

As a starting point, we describe the study of the electric field in the neighborhood of a nanoparticle using the electrostatic approximation [2]. The electric field corresponds to the plasmon particle. This model allows the description of the interaction between two plasmon particles. The interaction is extended to describe the plasmon fields propagating on a surface generating a wave behavior satisfying the Helmholtz equation where the wave number must have complex values in order to recover the traditional surface plasmon models. Controlling the random distribution of nanoparticles, we

analyze the correlation effects leading us to induce localization effects. This last statement is obtained by masking thin metal surface with two independent random array hole distributions. Controlling the scale factors, we modify the curvature of the correlation trajectory. The model is related with a speckle pattern emerging from a rough surface [5]. This configuration is similar to the configuration proposed by Reather for the coupling of plasmon fields. Experimental results are shown.

2. Analysis of plasmon particle

A nanoparticle is generated by a set of atoms; the plasmon particle corresponds with the surface current distribution of the atoms. The analysis is implemented applying the electrostatic approximation given by

$$\nabla^2\phi = 0, \tag{1}$$

where ϕ is the potential function. Using variable separation in Cartesian coordinates on the $x - y$ plane, the equation acquires the form

$$\frac{\partial^2\phi}{\partial x^2} + \frac{\partial^2\phi}{\partial y^2} = 0. \tag{2}$$

Proposing the solution as

$$\phi = X(x)Y(y), \tag{3}$$

we obtain the equation system

$$\ddot{X} - \alpha^2 X = 0 \tag{4a}$$

$$\ddot{Y} + \alpha^2 Y = 0, \tag{4b}$$

where the coupling constant α is a complex number having the form $\alpha = a + ib$. This condition is necessary because perturbing the field, it must acquire a propagating behavior as it is shown below. Solving for X, we have

$$X = c_1 e^{cx} e^{idx} + c_2 e^{cx} e^{-idx}, \tag{5}$$

and the solution for Y is given by

$$Y = D_1 e^{icy} e^{-dy}. \tag{6}$$

Then, the complete solution ϕ acquires the form

$$\phi = A e^{cx} e^{idx} e^{-dy} e^{icy}, \tag{7}$$

with $c < 0$ and $d > 0$. Eq. (7) represents the boundary condition for the plasmonic field.

2.1 Description for the interaction between plasmon particles

The model is extended to describe the propagation of the electric field. For this, we propose that the electrostatic approximation is no longer fulfilled, acquiring the form of the Helmholtz equation having the form

$$\nabla^2\phi + k^2\phi = 0. \tag{8}$$

Looking for propagation along the x-coordinate, the equation acquires the form

$$\frac{\partial^2\phi}{\partial x^2} + \frac{\partial^2\phi}{\partial y^2} + k^2\phi = 0, \tag{9}$$

where k is the complex wave number $k = k_1 + ik_2$. Proposing a solution of the form $\phi = X(x)Y(y)$, we obtain the equation system given by

$$\ddot{X} + \left(k^2 - h^2\right)X = 0 \tag{10a}$$

$$Y + \alpha^2 Y = 0, \tag{10b}$$

whose solution acquires the form

$$\phi_p = Me^{\gamma x}e^{i\Omega x}e^{-dy}e^{icy}, \tag{11}$$

this equation must recover the structure of the electrostatic approximation for a single nanoparticle.

From the previous solution, it is easy to identify its behavior. Along the y-coordinate the field is bounded by the exponential term, which remains unperturbed by the presence of a second particle; the interaction occurs mainly in the x-coordinate. This behavior may be generalized acquiring a wave effect. A balance relation between the complex wave number k and the constant coupling α can be predicted; this interaction decreases the evanescent term, and the propagating term becomes dominant. This interaction is sketched in **Figure 1**.

In **Figure 1a**, the electrostatic approximation is valid for a single nanoparticle; the wave behavior is generated by another set of particles interacting shown in **Figure 1c**.

Until this point we have described the generation of a wave propagating in the x-coordinate; this analysis can be extended to the propagation in the $x - y$ plane, which is analyzed in the following section.

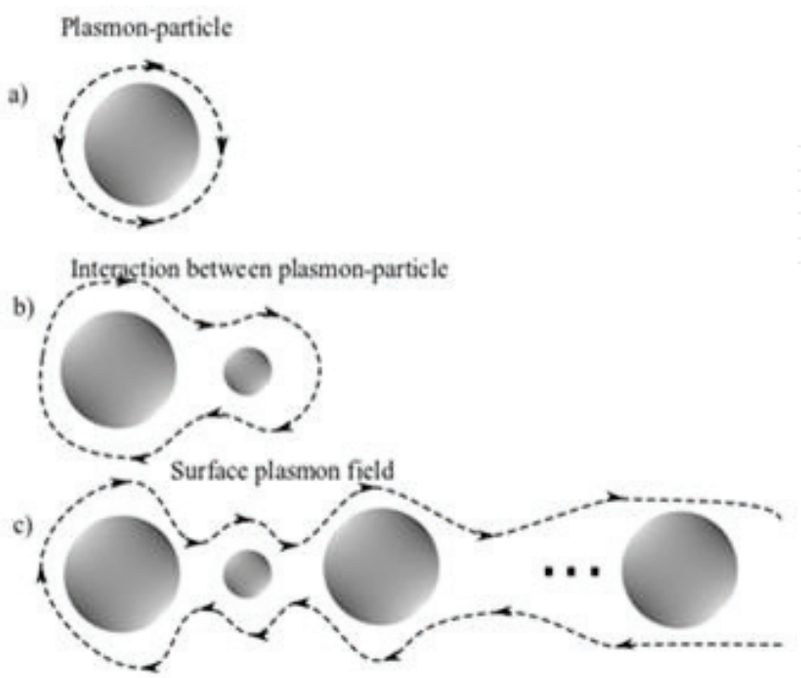

Figure 1.
(a) Localized electric field for a plasmon particle. (b) Interaction between two plasmon particles. (c) Sketch to describe the generation of a plasmon field in an array of nanoparticles.

3. Description statistics of correlation trajectories

In the present section, we describe the transfer of the statistical properties of an anisotropic two-dimensional random walk model to generate wave propagation on a metal surface, thus generating a curved surface plasmon mode. The model is conceptually simple. We describe a trajectory in a two-dimensional array, starting from a point P with coordinates $(0, 0)$. The random walk is characterized by a set of points randomly distributed, and the trajectory can be obtained from the correlation function corresponding to the flows of current probability. The statistical properties of a random distribution of points can be transferred to induce and control important physical effects. For example, it is known that the amplitude distribution of a speckle pattern follows Gaussian statistics [6, 7]. The statistic of the speckle pattern is matched with a random hole distribution, and it is transferred on a metal surface. The analysis is obtained by masking the surface metal which is considered to be formed by a set of square cells. The probability of a hole being present at the center of each cell is P; therefore, the probability of the absence of a hole is $(1 - P)$. The surface contains N cells, and the probability of the surface contains n-holes, assuming that a Bernoulli distribution is

$$P(n) = \binom{N}{n} P^n (1-P)^{N-n}. \tag{12}$$

When the number of cells N increases, the Bernoulli distribution tends to a Gaussian distribution of the form

$$\rho(x,y) = \frac{1}{\sqrt{2\pi\sigma^2}} e^{-\frac{x^2+y^2}{2\sigma^2}}, \tag{13}$$

where σ^2 is the variance. Interesting features can be identified by describing the self-correlation in this type of distribution. The simplest case occurs when two screens are superposed and, subsequently, one of them is rotated by a small angle. In order to understand the generation of the self-correlation trajectory, we focus on a single hole. In this case, it is evident that the hole follows a circular arc by joining all the points of constant probability and the complete correlation trajectory is a circle. The result in this case is shown in **Figure 2a**. The correlation trajectory can be controlled by inducing a scale factor in the distribution of random points. By

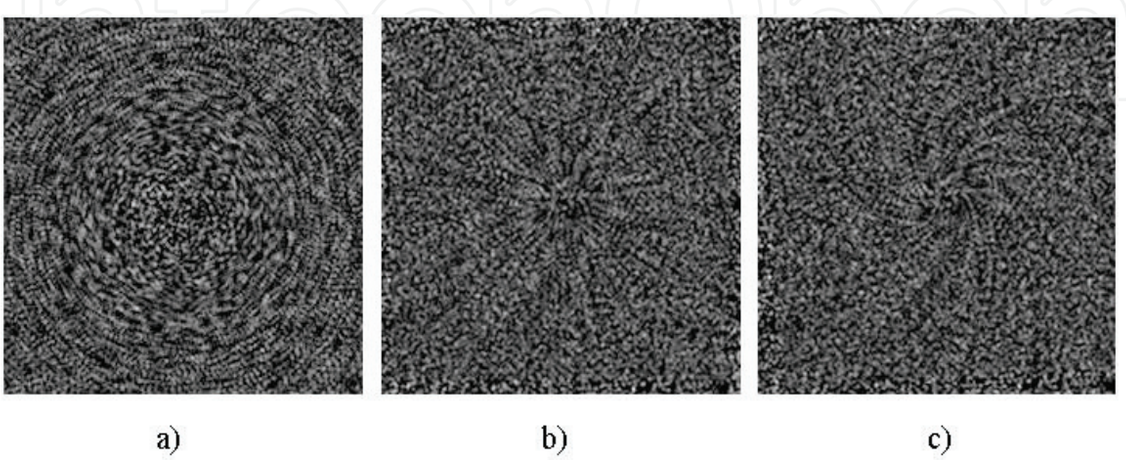

Figure 2.
(a) Set of points following a Gaussian distribution. (b) Correlation function between two Gaussian sets of points where one mask was rotated by a small angle. (c) Probability flow trajectories between two mask Gaussian points, one of them is scaled by approximately 95%, without rotation. (d) Same as in (c) but with a rotation of approximately 5°.

superposing the two screens again, it is evident that the scale factor shifts the point along a linear trajectory perpendicular to the regions of constant probability, which are sets of circles, as deduced from the argument of the Gaussian distribution. The analysis is presented in an equivalent way for a speckle pattern using the fact that both of them have the same probability distribution. In **Figure 2b**, we show these correlation trajectories. Finally, by introducing a small rotation, the linear trajectories are curved, as shown in **Figure 2c**.

This result can be explained as follows: the correlation function of two scaled and rotated surfaces have the form

$$\rho_1(x,y)\cdot\rho_2(x',y') = \frac{1}{\sqrt{2\pi}\sigma_1\sigma_2}\exp\left\{-\frac{x^2+y^2}{2\sigma_1^2}\right\} \times \exp\left\{-\left[\frac{d(x\cos\theta+y\,sen\theta]^2+[d(-x\,sen\theta+y\cos\theta)]^2}{2\sigma_2^2}\right\}\right. \tag{14}$$

Analyzing the argument of the exponential function as a quadratic form, it can be shown that the curves of constant correlation are ellipses, presenting a reference system where they acquire the canonical form

$$\frac{x^2}{a^2}+\frac{y^2}{b^2}=1. \tag{15}$$

The probability flows through the orthogonal trajectories between the two regions of constant probability, whose differential equation is given by

$$y'=\frac{b^2}{a^2}\frac{y}{x}. \tag{16}$$

Further, the corresponding solution is given by

$$y=cx^{\alpha}, \tag{17}$$

where c is an arbitrary constant and $\alpha=\frac{b^2}{a^2}$, which carries the information about the scale between the two probabilistic processes.

3.1 Graphical description and experimental implementation of the correlation trajectory

A fundamental part of the chapter consists of describing a method to generate surface plasmon fields propagating along predetermined trajectories. This can be obtained analyzing the correlation function between two screens where each one has a random hole distribution following a predetermined probability density function. This method has the characteristic that the correlation trajectory geometry presents a tunable curvature which allows the possibility to generate long-range surface plasmon.

An alternative model to generate the curved correlation trajectories is performed using a speckle pattern as it is shown in **Figure 4**.

The optical system that rotates the image can be a prism-type Dove. Modifying the illumination configuration using a convergent beam and changing the relative distance between the two speckle patterns obtained by shifting one mirror a scale factor are introduced. The irradiance superposition between the two speckle patterns generates the desired correlation trajectories. The speckle pattern is shown in **Figure 3**.

It is known that the irradiance function for the speckle pattern has associated a probability density function-type exponential decreasing function. The decreasing

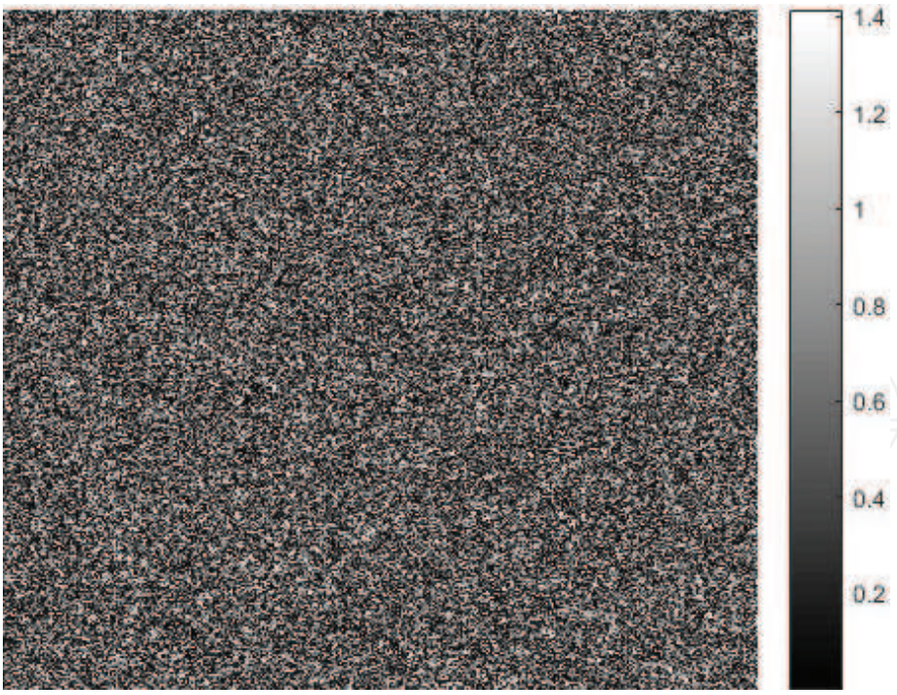

Figure 3.
Speckle pattern generated with a rough surface illuminated with a plane wave.

term can be matched with the decaying ratio of the plasmon mode. This configuration allows improving the generation of plasmon field avoiding the masking of the metal surface which must be made with lithography techniques. These comments represent novel applications of the speckle pattern.

The correlation trajectories generated will be implemented in the following section to describe the surface plasmon. By the fact that the correlation occurs in a curved trajectory, we expect the surface plasmon to present a magnetic behavior.

3.2 Generation of curved surface plasmon modes

The previous statistical description will be employed for the synthesis of surface plasmonic modes. The expression for the electric field of an elementary surface plasmonic mode propagating along the z-axis is given by

$$E(x,z) = \left(\hat{i}a + \hat{k}b\right) \exp\{-\alpha x\} \exp\{i\beta z\}, \tag{18}$$

where $\beta = \frac{w}{c}\left(\frac{\varepsilon_1\varepsilon_2}{\varepsilon_1+\varepsilon_2}\right)^{1/2} = \xi + i\eta$ is the dispersion relation function and ε_1, ε_2 represent the permittivity of the dielectric and metal, respectively. Rotating the reference system along the x-axis, the elementary surface plasmon mode acquires the form

$$E(x,z) = \left(\hat{i}a + \hat{j}bsin\theta + \hat{k}bcos\theta\right) \times \exp\{-\alpha_1 x\} \exp\{i\beta(zcos\theta + ysin\theta)\}. \tag{19}$$

Using the functional relation given by Eq. (17), the expression for the curved plasmonic mode is given by

$$E(x,y) = \left(\hat{i}a + \hat{j}bsin\theta + \hat{k}bcos\theta\right) \times \exp\{-\alpha_1 x\} \exp\{i\beta(y^{\alpha}cos\theta + ysin\theta)\}. \tag{20}$$

By means of the Maxwell equations, we can obtain the expression for the magnetic field and the energy flux given by the Poynting vector.

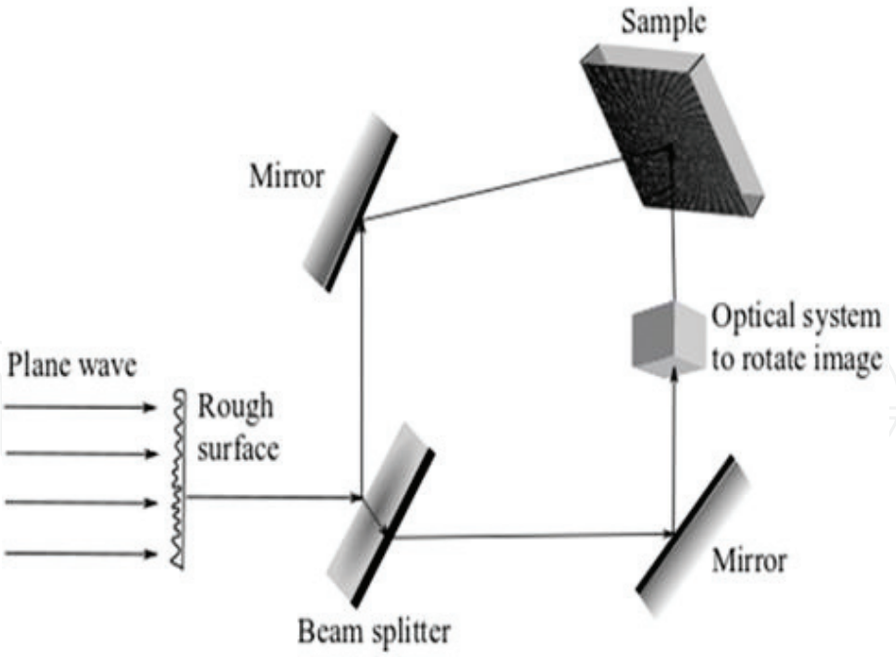

Figure 4.
Experimental setup to generate speckle correlation trajectories.

For the experimental setup, we propose to illuminate a thin flat Au film (thickness ∼20–40 nm) with a correlated speckle pattern as shown in **Figure 4**. The illumination consists in two speckle patterns: each one is visualized as a set of circular motes randomly distributed following a Gaussian probability density function. The wavelength is $\lambda = 1550$ nm. The geometrical parameters are agreeing with those reported in [8]. The correlation curve corresponds to the surface plasmonic mode given by Eq. (20). Notably, the statistical properties of the speckle pattern are transferred to the metal surface as the plasmonic mode propagating along the correlation trajectory. In order to allow the generation of a long-range curved plasmonic mode, the correlation length must be less than 2μ to guarantee resonance effects [9, 10]; this can be controlled with the roughness parameters of the surface implemented to generate the speckle pattern avoiding the power decay along the correlation trajectory. The experimental setup is sketched in **Figure 5**.

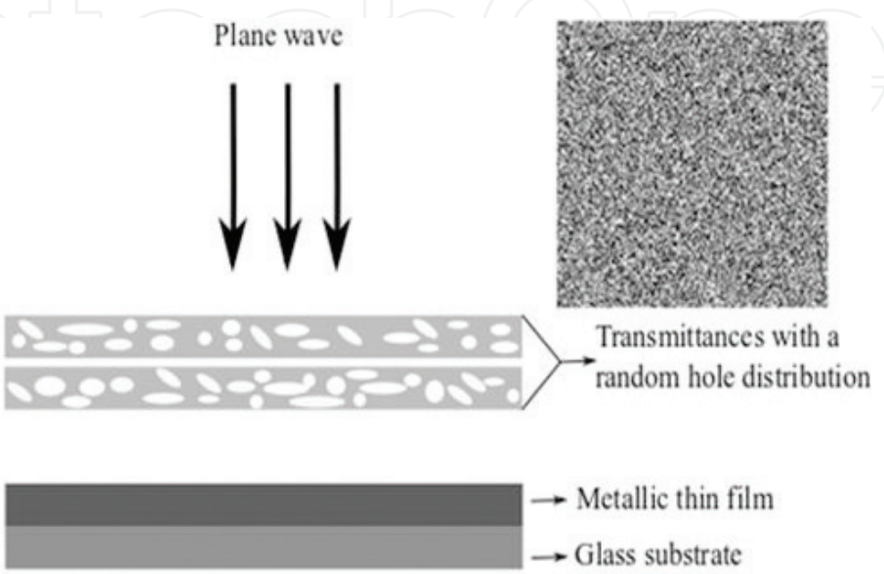

Figure 5.
Masked metal surface: The typical wavelength is IR.

The analysis presented can be extended to other plasmonic configurations which are presented in the following section.

4. Propagation in a tandem array of thin metal films

The natural extension of the analysis presented is the transfer of the plasmonic mode to a tandem array of thin metal surface, shown in **Figure 6**. This is possible using the evanescent behavior along the x-axis of the curved surface plasmon field. This behavior has been implemented to generate an optical field redistribution propagating along an optical waveguide array [11]. In this model, the evanescent character is used to tunnel the optical field.

The transmission of the plasmonic mode satisfies the following system of differential equations:

$$i\frac{dE_n}{dz} + \beta E_n + C_{n+1}E_{n+1} + C_{n-1}E_{n-1} = 0 \tag{21a}$$

$$n = 1, 2, 3\ldots, \tag{21b}$$

where β is the dispersion relation function and C_i represents the coupling constant, which depends on the relative separation between neighborhood surfaces [12]. The solution of the previous equation is similar to that presented in [11]; however, to associate a physical meaning to the coupling constant C_i, we present the analysis of two thin metal films.

The simplest case occurs when the system is formed by two thin metal films separated by a dielectric medium whose thickness must be less than 50 nm. The evanescent decay depends on the modulus of the permittivity quotient [13], and at this thickness is possible to generate tunneling effects [11]. Subsequently, the system of Eq. (21a) acquires the simple form

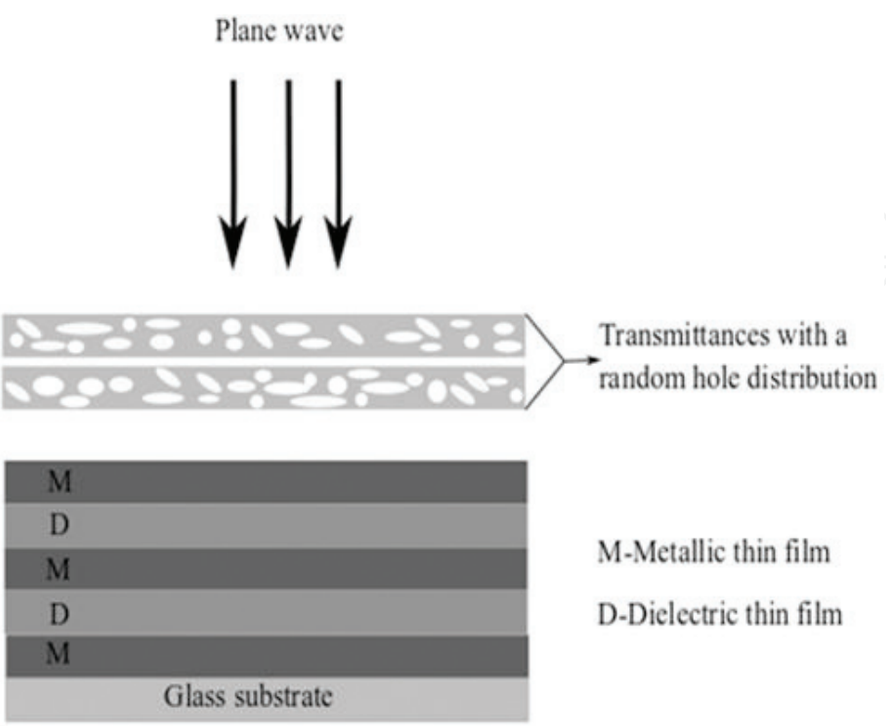

Figure 6.
Tandem array to propagate the plasmon field: the width of the metal is $20 - 40$ *nm and that dielectric film is* $20 - 40$ *nm.*

$$i\frac{dE_1}{dz} + \beta E_1 + C_2 E_2 = 0, \tag{22a}$$

$$i\frac{dE_2}{dz} + \beta E_2 + C_1 E_1 = 0. \tag{22b}$$

Rewriting it in matrix form, we obtain

$$i\begin{pmatrix} \frac{dE_1}{dz} \\ \frac{dE_2}{dz} \end{pmatrix} = -\begin{pmatrix} \beta & c_2 \\ c_1 & \beta \end{pmatrix}. \tag{23}$$

It can be deduced that, as a consequence of the energy conservation, the matrix structure must be symmetric. This indicates that $c_1 = c_2 = c$, and the general solution is

$$\begin{pmatrix} E_1 \\ E_2 \end{pmatrix} = d_1\begin{pmatrix} \xi_1 \\ \xi_2 \end{pmatrix}\exp(\lambda_1 z) + d_2\begin{pmatrix} \eta_1 \\ \eta_2 \end{pmatrix}\exp(\lambda_2 z), \tag{24}$$

where d_i represents arbitrary constants and $\xi_{1,2}$ and $\eta_{1,2}$ represent the eigenvectors with eigenvalues $\lambda_{1,2}$ satisfying the characteristic equation depending on the coupling constant:

$$\lambda_{1,2} = \beta \pm c. \tag{25}$$

Moreover, it is known that the eigenvectors must be complex [14]. Subsequently, without loss of generality, the solution can be rewritten as

$$\begin{pmatrix} E_1 \\ E_2 \end{pmatrix} = d_1\begin{pmatrix} 1 \\ i \end{pmatrix}\exp(\lambda_1 z), \tag{26}$$

which indicates that the shift generated between each plasmon mode presents similar features as the coupling mode theory [12]. This analysis leads to the expression for the plasmonic mode as

$$E_1 = A\,\vec{\xi}\,\exp(-|\alpha x|)\exp(i\beta s) \tag{27a}$$

$$E_2 = iA\,\vec{\xi}\,\exp(-|\alpha x|)\exp(i\beta s), \tag{27b}$$

where $\vec{\xi}$ is a unit vector tangent to the correlation curve and s is the arc length on the same curve; we remark that the correlation trajectory is given by Eq. (20).

Eq. (24) describes the evanescent coupling through a tandem array of thin metal films. Notably, the boundary conditions of the electric field indicate that the geometry of the plasmon field generated in the first thin metal film must be preserved in all the surfaces. This shows that the transmission of the curved plasmonic mode allows inducing magnetic properties in the system [15–18].

5. Conclusions

The statistical properties of the distribution of random holes or equivalently the speckle pattern were transferred to a metal surface to stablish the conditions to generate long-range curved plasmonic modes. In the case of hole distribution, this

can be implemented by masking a thin metal film with two screens that allows controlling the correlation trajectory whose geometry corresponds to a curved long-range surface plasmonic mode. Another possibility was illuminating the metal thin film with two correlated speckle patterns. An important consequence of these configurations is that the set of curved surface plasmonic modes presents a vortex structure that allows to induce magnetic properties [17]. Using the evanescent character of the plasmon modes, the electric field was transferred to the propagation in a tandem array of thin metal films offering applications to design photonic crystals with tunable and localized magnetic properties.

The theoretical point of view presented in this study allows incorporating other effects such as percolation effects which consist in propagating the electric field through random structures. The main characteristic is that the plasmon field presents fractal properties which are the origin of interesting magnetic properties implicit in the curved trajectory of the set of plasmonic modes; more details can be found in [18]. The model presented can be extended by implementing different hole distribution geometries which modify the plasmonic resonance effects. Notably, the curved trajectories have associated focusing regions, and, subsequently, the corresponding magnetic singularity offers the possibility of implementation in the generation of plasmonic magnetic mirrors.

Finally, we remark that the analysis presented offers applications to photonic crystal as a metamaterial design [19–23] since breaking the periodicity or incorporating another type of metal on a selected region is similar to doping the structure and then is possible to induce localization effects. The excitation of plasmon fields using a speckle patterns offers the possibility to incorporate the tunable behavior of the correlation trajectory offering interesting applications in the development of plasmonic antennas and synthesis of accelerating plasmon modes [21], extending the plasmonic optical models.

Acknowledgements

The authors MATR and MVM are very grateful to CONACyT for their support.

DOI: http://dx.doi.org/10.5772/intechopen.81931

Author details

Gabriel Martinez Niconoff[1]*, Marco Antonio Torres Rodriguez[1], Mayra Vargas Morales[1] and Patricia Martinez Vara[2]

1 Departamento de Optica, Instituto Nacional de Astrofisica, Optica y Electronica (INAOE), Puebla, Mexico

2 Departamento de Ingenierias, Benemerita Universida Autonoma de Puebla (BUAP), Puebla, Mexico

*Address all correspondence to: gmartin@inaoep.mx

References

[1] Brinks D, Castro-Lopez M, Hildner R, Van Hulst NF. Plasmonic antennas as design elements for coherent ultrafast nanophotonics. Proceedings of the National Academy of Sciences. 2013; **110**(46):18386-18390

[2] Aroca R. Surface-Enhanced Vibrational Spectroscopy. J. Wiley and Sons; 2006

[3] Berger V. Nonlinear photonic crystals. Physical Review Letters. 1998; **81**:4136-4139

[4] O'Brien S, Pendry JB. Photonic band-gap effects and magnetic activity in dielectric composites. Journal of Physics: Condensed Matter. 2002;**14**(15):4035-4044

[5] Raether H. Surface Plasmons on Smooth and Rough Surfaces on Gratings. Berlin Heidelberg: Springer-Verlag; 1988

[6] Spitzer F. Principles of Random Walk. New York: Springer-Verlag; 2001

[7] Goodman JW. Statistical properties of laser speckle patterns. In: Laser Speckle and Related Phenomena. Berlin Heidelberg: Springer; 1975. pp. 9-75

[8] Martínez Niconoff G, Martínez Vara P, Diaz Gonzalez G, Silva Barranco J, Carbajal Dominguez A. Surface plasmon singularities. International Journal of Optics Special Issue of Nanoplasmonics and Metamaterials. 2012;**2012**:7

[9] Jung K-Y et al. Au/SiO_2 Nanoring Plasmon waveguides at optical communication band. Journal of Lightwave Technology. 2007;**25**(9): 2757-2765

[10] Ahmadivand1 A, Golmohammadi S. Electromagnetic plasmon propagation and coupling through gold nanoring heptamers: A route to design optimized telecommunication photonic nanostructures. Applied Optics. 2004; **53**(18):3832-3849

[11] Martin L, Di Giuseppe G, Perez Leija A, Keil R, Dreisow F, Heinrich M, et al. Anderson localization in optical waveguide arrays with off-diagonal coupling disorder. Optics Express. 2011; **19**(14):13636-13646

[12] Rodrıguez-Lara BM, Soto-Eguibar F, Zarate Cardenas A, Moya-Cessa HM. A classical simulation of nonlinear Jaynes–Cummings and Rabi models in photonic lattices. Optics Express. 2013;**21**(10): 12888

[13] Lee SY, Park J, Kang M, Lee B. Highly efficient plasmonic interconnector based on the asymmetric junction between metal-dielectric-metal and dielectric slab waveguides. Optics Express. 2011;**19**(10):9562-9574

[14] Hirsch MW, Smale S, Devaney RL. Differential Equations, Dynamical Systems, and an Introduction to Chaos. USA: Academic press, Elsevier; 2012

[15] McGurn AR, Maradudin AA, Celli V. Localization effects in the scattering of light from a randomly rough grating. Physical Review B. 1985;**31**(8):4866

[16] Zia R, Schuller JA, Brongersma ML. Near-field characterization of guided polariton propagation and cutoff in surface plasmon waveguides. Physics Review B. 2006;**74**:165415

[17] Engelhardt M, Langfeld K, Reinhardt H, Tennert O. Deconfinement in SU(2) Yang-Mills theory as a center vortex percolation transition. Physics Review D. 2000;**61**: 054504

[18] Enders D, Nagao T, Pucci A, Nakayama T, Aono M. Surface-enhanced ATR-IR spectroscopy with

interface-grown plasmonic gold-island films near the percolation threshold. Physical Chemistry Chemical Physics. 2011;**13**(11):4935-4941

[19] Maigyte L, Staliunas K. Spatial filtering with photonic crystals. Applied Physics Reviews. 2015;**2**(1):011102

[20] Zheng X, Smith W, Jackson J, Moran B, Cui H, Chen D, et al. Multiscale metallic metamaterials. Nature Materials. 2016;**15**:1100-1106

[21] Zhang P, Hu Y, Cannan D, Salandrino A, Li T, Morandotti R, et al. Generation of linear and nonlinear nonparaxial accelerating beams. Optics Letters. 2012;**37**(14):2820-2822

[22] Yeh P. Introduction to Photorefractive Nonlinear Optics. New York: J. Wiley and Sons; 1993. pp. 47-61

[23] Prasad P. Nanophotonics. Hoboken, New Jersey: J. Wiley and sons; 2004